Sensors and Materials, Vol. 38, No. 6 (2026) 3015–3022
MYU Tokyo

S & M 4484

Effects of Oxygen Flow Rate on Optoelectronic Characteristics of SnO_2 Thin Films for Application to Optical Sensors

Chi-Fan Liu, Yun Ho, and Tao-Hsing Chen*

Department of Mechanical Engineering, National Kaohsiung University of Science and Technology, Kaohsiung City 807, Taiwan, No. 415, Jiangong Rd., Sanmin Dist., Kaohsiung City 807618, Taiwan

(Received January 27, 2026; accepted March 19, 2026)

Keywords: SnO_2, electrical property, RF sputtering, optical property, oxygen flow rate

In this study, tin oxide (SnO_2) thin films were deposited on glass substrates by RF magnetron sputtering, with process parameters optimized by adjusting the oxygen flow rate. Subsequently, thermal treatment was performed at various temperatures in a vacuum environment. The thickness, electrical conductivity, optical transmittance, and figure of merit (FOM) of the films were analyzed. The results indicate that the films deposited with an oxygen flow rate of 5 sccm, a sputtering power of 80 W, and a deposition time of 30 min, followed by annealing at 200 °C, exhibited the highest performance. Specifically, the films achieved a minimum resistivity of 3.19 × 10^{-2} Ω·cm and an optimal FOM of 7.43 × 10^{-5} $Ω^{-1}$. These findings demonstrate excellent optoelectronic properties, suggesting high potential for applications in optoelectronic sensor materials.

1. Introduction

Thin films represent a unique state of matter extensively utilized in emerging devices such as microelectronics, sensors, solar cells, and liquid crystal displays (LCDs).[1–4] With the rapid advancement of thin-film science, various preparation techniques have been developed, ranging from vacuum evaporation to ion plating, sputtering, and chemical vapor deposition (CVD).[5–9]

Transparent conducting oxides (TCOs) are critical optoelectronic materials that combine excellent electrical conductivity with high optical transparency, making them widely applicable in solar cells, flat-panel displays, thin-film transistors (TFTs), and organic light-emitting diodes (OLEDs).[3] TCO films exhibit high carrier concentration and low resistivity while maintaining high transparency in the visible light spectrum. To achieve high transmittance, materials with a bandgap greater than 3 eV, such as In_2O_3, TiO_2, ZnO, SnO_2, and CdO, are typically selected.[10–14] These materials exhibit semiconducting characteristics while maintaining optical clarity, further expanding their utility in optoelectronics. While indium tin oxide (ITO) is currently the industry standard, its widespread application is limited by the scarcity and high cost of indium, as well as its relative instability in harsh environments. Consequently, tin oxide (SnO_2) has emerged as a highly promising alternative. As an n-type semiconductor with a wide

*Corresponding author: e-mail: thchen@nkust.edu.tw
https://doi.org/10.18494/SAM6229

ISSN 0914-4935
https://myukk.org/

direct bandgap ($Eg \approx 3.6$ eV), SnO_2 offers several distinct advantages, for example, abundance and low cost, chemical and thermal stability, and mechanical durability.[15–18]

The optoelectronic performance of SnO_2 thin films is highly sensitive to their stoichiometric composition and crystal structure, which are governed by deposition parameters. Among these, the oxygen flow rate during sputtering plays a critical role. Oxygen vacancies act as shallow donors that contribute to electrical conductivity; however, excessive oxygen can lead to a decrease in carrier concentration while improving optical transparency. Therefore, identifying the optimal oxygen flow rate is essential to achieving the best balance between electrical and optical properties, that is, the figure of merit (FOM).[19]

Despite numerous studies on SnO_2-based materials, achieving a synergistic optimization of electrical conductivity and optical clarity remains a challenge owing to the complex interplay between oxygen vacancies and structural defects. The primary objective of this study is to systematically investigate the effects of oxygen flow rate and post-annealing temperature on the optoelectronic characteristics of SnO_2 thin films deposited by RF magnetron sputtering.

We hypothesize that the precise modulation of the oxygen-to-argon ratio during deposition can effectively tailor the density of oxygen vacancies, which act as shallow donors, thereby enhancing the carrier concentration and reducing resistivity without compromising the optical bandgap. Furthermore, it is anticipated that subsequent thermal treatment will improve the crystallinity and surface morphology, leading to a superior FOM. By analyzing the correlation between deposition parameters and the resulting film properties—including thickness, resistivity, Hall mobility, and visible-light transmittance—in this work, we aim to identify the optimal processing window for high-performance SnO_2 films suitable for advanced optoelectronic sensor applications.

2. Experimental Procedure

The SnO_2 target used in this experiment was purchased from Summit International Development Co., Ltd., and Corning glass was employed as the substrate. The substrate was sequentially cleaned in deionized (DI) water, isopropyl alcohol (IPA), and acetone, followed by drying in an oven at 90 ℃. Sputtering was conducted at a power of 80 W and a working pressure of 6 mTorr with various oxygen flow rates. Post-deposition thermal treatment was performed at temperatures ranging from 200 to 500 ℃. A surface profilometer (alpha-step) was used to measure the thickness of the films. The total transmittance in the visible range (380–780 nm) was measured using a UV–Vis spectrophotometer. The resistivity, carrier concentration, and Hall mobility were measured at room temperature using a Hall effect measurement system (van der Pauw method).

3. Results and Discussion

3.1 Film thickness

Film thickness was measured using a surface profilometer (alpha-step). As shown in Table 1, the thin films have the same thickness even with different O_2 flow rates.[20]

Table 1
Thickness of the thin films.

Sputtering power (W)	Gas flow (sccm)	Working pressure (mtorr)	Sputtering time (min)	Thickness (nm)
80	Ar: 30, O_2: 0	6	30	60.82
80	Ar: 30, O_2: 1	6	30	62.16
80	Ar: 30, O_2: 5	6	30	61.97
80	Ar: 30, O_2: 10	6	30	62.50

3.2 Analysis of electrical properties

Figures 1–4 present the results of the electrical analyses of SnO_2 films under different annealing temperatures and O_2 flow rates. The lowest resistivity of 3.19×10^{-2} Ω·cm was observed at an O_2 flow rate of 5 sccm. The literature suggests that introducing an appropriate amount of O_2 during sputtering results in a higher concentration of oxygen vacancies, which increases carrier concentration and conductivity. However, excessive O_2 flow causes oxygen to fill these vacancies, reducing carrier concentration and increasing resistivity. Furthermore, as the annealing temperature increases, the oxidation of SnO_2 becomes more complete, further reducing oxygen vacancies and leading to higher resistivity.

The electrical resistivity (ρ) of the SnO_2 thin films is governed by the relationship $\rho = 1/(ne\mu)$, where n is the carrier concentration, e is the elementary charge, and μ is the Hall mobility. The experimental results in Figs. 1–4 reveal that the variations in resistivity are a result of the competing effects of these two parameters under different processing conditions. At lower oxygen flow rates (e.g., 5 sccm), a higher density of oxygen vacancies is maintained, resulting in a high carrier concentration. Thermal treatment promotes grain growth and improves the crystallinity of the SnO_2 lattice. Larger grains reduce the density of grain boundaries, thereby decreasing the potential barriers that impede carrier transport and enhancing mobility. The minimum resistivity of 3.19×10^{-2} Ω·cm achieved at 200 °C with 5 sccm oxygen flow represents the point where the product of n and μ is maximized. At temperatures exceeding 300 °C, the resistivity begins to rise again. This is attributed to the "over-oxidation" of the film, where further reduction in carrier concentration (owing to the loss of oxygen vacancies) outweighs the minor gains in mobility through improved crystallinity.

3.3 Transmittance analysis

Regarding transmittance (Figs. 5–8), lower O_2 flow rates result in higher concentrations of SnO_2 phases or oxygen vacancy defects, which reduces transparency. As the O_2 flow rate increases, these defects are minimized, significantly enhancing transmittance. The optical bandgap Eg can also represent film transparency. Materials with $Eg > 3$ eV are classified as wide-bandgap semiconductors. The bandgap is calculated using the Tauc plot formula:[21,22]

$$(\alpha h\upsilon)^2 = A(h\upsilon - Eg), \tag{1}$$

where A is a constant, α is the absorption coefficient, and $h\upsilon$ is the incident photon energy. Overall, the four groups of samples showed an increasing trend in bandgap within the annealing

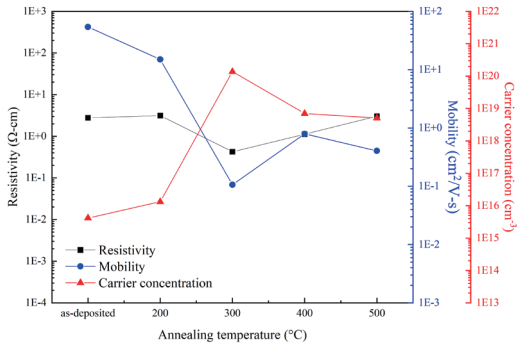

Fig. 1. (Color online) Electrical properties of SnO_2 thin films deposited at zero oxygen flow rate under different annealing temperatures.

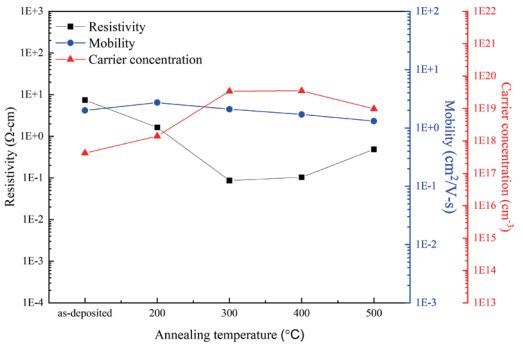

Fig. 2. (Color online) Electrical properties of SnO_2 thin films deposited at 1 sccm oxygen flow rate under different annealing temperatures.

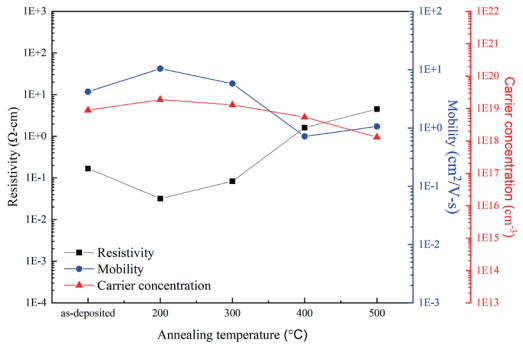

Fig. 3. (Color online) Electrical properties of SnO_2 thin films deposited at 5 sccm oxygen flow rate under different annealing temperatures.

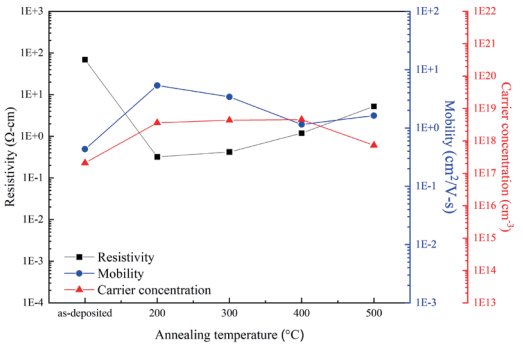

Fig. 4. (Color online) Electrical properties of SnO_2 thin films deposited at 10 sccm oxygen flow rate under different annealing temperatures.

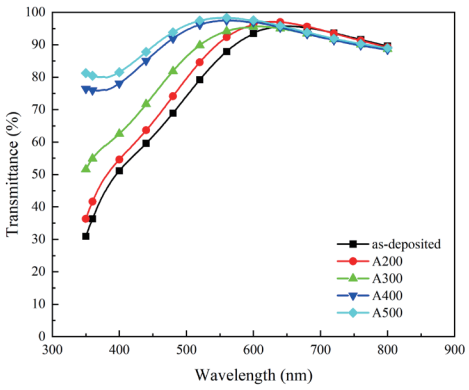

Fig. 5. (Color online) Optical transmittance of SnO_2 thin films deposited at zero oxygen flow rate under different annealing temperatures.

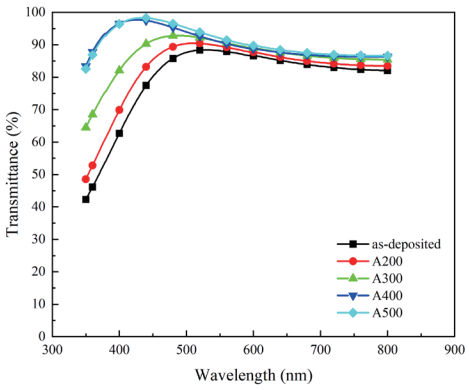

Fig. 6. (Color online) Optical transmittance of SnO_2 thin films deposited at 1 sccm oxygen flow rate under different annealing temperatures.

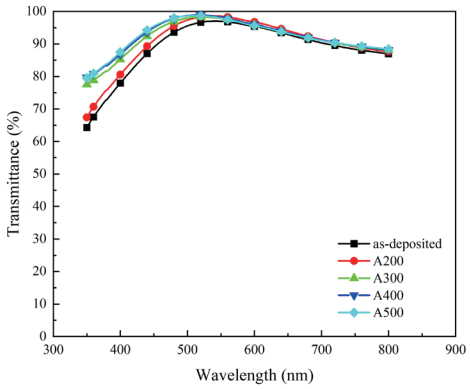

Fig. 7. (Color online) Optical transmittance of SnO_2 thin films deposited at 5 sccm oxygen flow rate under different annealing temperatures.

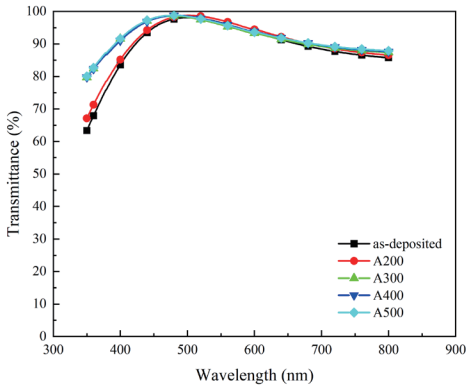

Fig. 8. (Color online) Optical transmittance of SnO_2 thin films deposited at 10 sccm oxygen flow rate under different annealing temperatures.

Table 2
Energy gap (*Eg*) of thin films deposited with various O_2 flow rates.

	Energy Gap (eV)			
Annealing temperature (°C)	Ar: 30	O_2: 1	O_2: 5	O_2: 10
as-deposited	3.06	3.1	3.59	3.53
200	3.21	3.24	3.62	3.57
300	3.52	3.5	3.71	3.64
400	3.8	3.68	3.73	3.66
500	3.84	3.68	3.73	3.67

tenperature range of 200–500 °C (Table 2). All measured bandgap values were above 3 eV, consistent with typical wide-bandgap semiconductor characteristics.

3.4 FOM

The performance of TCO films is often evaluated using the FOM, defined as the ratio of transmittance to resistance:[23–25]

$$\varnothing_{TC} = \frac{T_{av}^{10}}{R_{sh}}, \tag{2}$$

where T_{av} is the average optical transmittance and R_{sh} is the sheet resistance expressed in Ω^{-1}. Since the FOM is proportional to the tenth power of transmittance, transmittance has a dominant impact. An optimal FOM requires both high transmittance and low resistivity. As shown in Fig. 9, the highest FOM was achieved at an O_2 flow rate of 5 sccm and an annealing temperature of 200 °C.

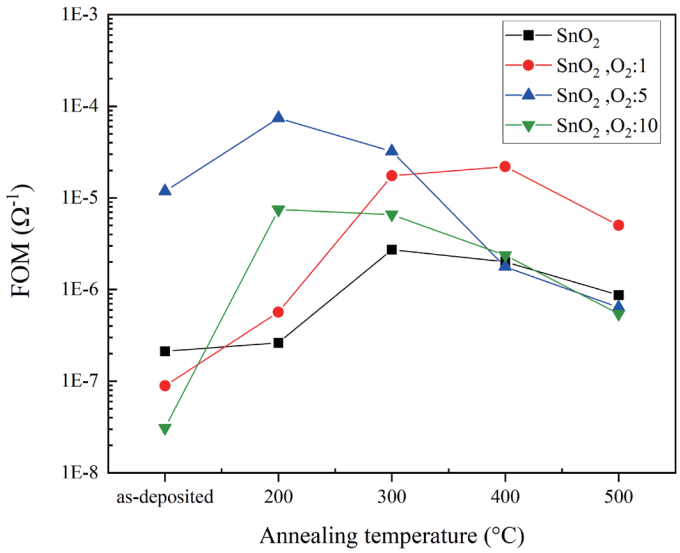

Fig. 9. (Color online) FOM of SnO_2 thin films annealed at different temperatures.

4. Conclusions

1. The thickness of SnO_2 thin films remained relatively constant regardless of O_2 flow rate or annealing temperature.
2. The minimum resistivity of 3.19×10^{-2} Ω·cm was obtained with 5 sccm O_2 flow and 200 °C annealing.
3. All samples exhibited average transmittance exceeding 80% and bandgap values above 3 eV.
4. The optimal FOM of 7.43×10^{-5} Ω^{-1} was achieved under the 5 sccm O_2 flow and annealing temperature of 200 °C, primarily owing to the superior electrical conductivity of the SnO_2 thin films.

In this study, SnO_2 transparent conductive thin films were successfully deposited by RF magnetron sputtering, and the effects of the oxygen flow rate on their physical properties were systematically investigated.

Acknowledgments

This paper was completed as part of Research Project NSTC114-2637-E-992 -004, which is supported by the National Science and Technology Council of Taiwan. The authors would like to express their gratitude to the National Science and Technology Council for its support, which enabled the smooth completion of this research. The authors also gratefully acknowledge the use of EM000700 of NSTC 114-2731-M-006-001 belonging to the Core Facility Centre of National Cheng Kung University.

References

1 T. H. Chen and C. L. Yang: Opt. Quant. Electron. **48** (2016) 533. https://doi.org/10.1007/s11082-016-0808-3
2 J. Schmitz: Surf. Coat. Technol. **343** (2018) 83. https://doi.org/10.1016/j.surfcoat.2017.11.013
3 W. N. Wang, T. D. Chang, and T. H. Chen: Sens. Mater. **36** (2024) 3757. https://doi.org/10.18494/SAM5049
4 A. Zeumault, J. E. Mendez, and J. Brewer: J. Soc. Inf. Disp. **32** (2024) 121. https://doi.org/10.1002/jsid.1274
5 C. H. Yu, S. T. Wicaksono, S. T. Wang, and T. H. Chen: Sens. Mater. **37** (2025) 1825. https://doi.org/10.18494/SAM5316
6 T. H. Chen, C. C. Chiang, and T. Y. Chen: Microsyst. Technol. **32** (2017) 1687. https://doi.org/10.1007/s00542-015-2689-y
7 M. Purica, E. Budianu, E. Rusu, M Danila, and R. Gavrila: Thin Solid Films **403–404** (2002) 485. https://doi.org/10.1016/S0040-6090(01)01544-9
8 H. Pedersen, S. T. Barry, and J. Sundqvist: J. Vac. Sci. Technol. A **39** (2021) 051001. https://doi.org/10.1116/6.0001125
9 J. F. Li, Z. Liu, Y. Zhang, B. Jia, W. Xu, X. Liu, L. Ji, A. Wang, C. Sun, and H. Li: Ceram. Int. **50** (2024) 43032. https://doi.org/10.1016/j.ceramint.2024.08.154
10 C. F. Liu, T. H. Chen, and Y. S. Huang: Sen. Mater. **32** (2020) 2321. https://doi.org/10.18494/SAM.2020.2867
11 T. H. Chen , M. W. Wang, C. L. Yang, and Y. S. Huang: Microsyst. Technol. **25** (2019) 2109. https://doi.org/10.1007/s00542-019-04360-z
12 M. Y. Yen, T. H. Chen, P. H. Lai, S. L. Tu, and Y. H. Shen: Sen. Mater. **33** (2021) 3941. https://doi.org/10.18494/SAM.2021.3706
13 A. M. Mostafa and A. A. Menazea: Radiat. Phys. Chem. **176** (2020) 109020. https://doi.org/10.1016/j.radphyschem.2020.109020
14 C. F. Liu, S. C. Shi, T. H. Chen, and G. L. Guo: Sens. Mater. **34** (2022) 4127. https://doi.org/10.18494/SAM4133
15 A. K. Gangwar, R. Godiwal, J. Jaiswal, V. Baloria, P. Pal, G. Gupta, and P. Singh: Vacuum **177** (2020) 109353. https://doi.org/10.1016/j.vacuum.2020.109353
16 A. Kania, M. M. Szindler, M. Szindler, Z. Brytan, and W. Łoński: Materials **17** (2024) 3348. https://doi.org/10.3390/ma17133348
17 Y. Xu, L. Zheng, C. Yang, W. Zheng, X. Liu, and J. Zhang: ACS Appl. Mater. Interfaces **12** (2020) 20704. https://doi.org/10.1021/acsami.0c04398
18 Y. Jang, H. Lee, and K. Char: AIP Advances **10** (2020) 035011. https://doi.org/10.1063/1.5143468
19 R. Ramarajan, N. Purushothamreddy, R. K. Dileep, M. Kovendhan, G. Veerappan, K. Thangaraju, and D. P. Joseph: Solar Energy **211** (2020) 547. https://doi.org/10.1016/j.solener.2020.09.042
20 Y. Tao, B. Zhu, Y. Yang, J. Wu, and X. Shi: Mater. Chem. Phys. **250** (2020) 123129. https://doi.org/10.1016/j.matchemphys.2020.123129.
21 T. Minami, H. Nanto, and S. Takata: J. Appl. Phys. **24** (1985) L605. https://doi.org/10.1143/JJAP.24.L605
22 W. N. Wang, T. D. Chang, and T. H. Chen: Sens. Mater. **36** (2024) 3757. https://doi.org/10.18494/SAM5049
23 D. Kim: Mater. Lett. **64** (2010) 668. https://doi.org/10.1016/j.matlet.2009.12.032
24 C. Y. Lin, T. H. Chen, S. L. Tu, Y. H Shen, and J. T. Huang: Opt Quant Electron **50** (2018) 169. https://doi.org/10.1007/s11082-018-1430-3
25 C. H. Yu, S. T. Wicaksono, S. T. Wang, and T. H. Chen: Sens. Mater. **37** (2025) 1825. https://doi.org/10.18494/SAM5316

About the Authors

Chi-Fan Liu received his M.D. degree from the University of the Incarnate Word, U.S.A., in 2002. Since 2004, he has been an associate professor at Feng Chia University, Taiwan. Since 2019, he has been the head of Yuchi Township, Nantou County, Taiwan. Now, he is a Ph.D. graduate student at National Kaohsiung University of Science and Technology, Department of Mechanical Engineering, Kaohsiung, Taiwan. His research interests are in thin films, sports science, bioengineering, and sensors.

Yun Ho received her B.S. degree from National Kaohsiung University of Science and Technology, Taiwan, where she is currently studying for her M.S. degree. Her research interests include TCO thin films, materials engineering, and sensors.

Tao-Hsing Chen received his B.S. degree from National Cheng Kung University, Taiwan, in 1999, and his M.S. and Ph.D. degrees from the Department of Mechanical Engineering, National Cheng Kung University, in 2001 and 2008, respectively. From August 2008 to July 2010, he was a postdoctoral researcher at the Centre for Micro/Nano Science and Technology, National Cheng Kung University. In August 2010, he became an assistant professor at National Kaohsiung University of Applied Sciences (currently National Kaohsiung University of Science and Technology), Taiwan. Since 2016, he has been a professor at National Kaohsiung University of Science and Technology. His research interests include metal materials, TCO thin films, thermal sensors, and photosensors. (thchen@nkust.edu.tw)